

## ASSEMBLY OF PROTOPLANETARY DISKS AND INCLINATIONS OF CIRCUMBINARY PLANETS

FRANCOIS FOUCART<sup>1</sup> AND DONG LAI<sup>2</sup>

<sup>1</sup>Canadian Institute for Theoretical Astrophysics, University of Toronto, Toronto, Ontario M5S 3H8, Canada

<sup>2</sup>Department of Astronomy, Cornell University, Ithaca, NY 14853, USA

*Draft version June 19, 2021*

### ABSTRACT

The *Kepler* satellite has discovered a number of transiting planets around close binary stars. These circumbinary systems have highly aligned planetary and binary orbits. In this paper, we explore how the mutual inclination between the planetary and binary orbits may reflect the physical conditions of the assembly of protoplanetary disks and the interaction between protostellar binaries and circumbinary disks. Given the turbulent nature of star-forming molecular clouds, it is possible that the gas falling onto the outer region of a circumbinary disk and the central protostellar binary have different axes of rotation. Thus, the newly assembled circumbinary disk can be misaligned with respect to the binary. However, the gravitational torque from the binary produces a warp and twist in the disk, and the back-reaction torque tends to align the disk and the binary orbital plane. We present a new, analytic calculation of this alignment torque, and show that the binary-disk inclination angle can be reduced appreciably after the binary accretes a few percent of its mass from the disk. Our calculation suggests that in the absence of other disturbances, circumbinary disks and planets around close (sub-AU) stellar binaries, for which mass accretion onto the proto-binary is very likely to have occurred, are expected to be highly aligned with the binary orbits, while disks and planets around wide binaries can be misaligned. Measurements of the mutual inclinations of circumbinary planetary systems can provide a clue to the birth environments of such systems.

*Subject headings:* accretion, accretion disks – hydrodynamics – planetary systems: protoplanetary disks – stars: binary

### 1. INTRODUCTION

The extremely precise photometry and nearly continuous observations provided by the *Kepler* satellite have led to the discovery of a number of transiting planetary systems around stellar binaries. At the time of this writing, six such circumbinary systems are known, including Kepler-16 (with stellar binary period of 41 days and planet orbital period of 229 days; Doyle et al. 2011), Kepler-34 (28 d, 289 d), Kepler-35 (21 d, 131 d; Welsh et al. 2012), Kepler-38 (19 d, 106 d; Orosz et al. 2012a), Kepler-47 (stellar binary orbit 7.45 d, with two planets of periods 49.5 d and 303.2 d; Orosz et al. 2012b), and KIC 4862625 (20 d, 138 d; Schwamb et al. 2012, Kostov et al. 2012). The stars in these systems have masses of order of the mass of the sun or smaller, and the planets have radii ranging from 3 earth radii (Kepler-47b) to 0.76 Jupiter radii (Kepler-34b).

By virtue of their detection methods, all the Kepler circumbinary systems have highly aligned planetary and stellar orbits, with the mutual orbital inclinations constrained between  $\Theta \sim 0.2^\circ$  (for Kepler-38b) and  $\Theta \lesssim 2^\circ$  (Kepler-34b and Kepler-35b). In Kepler-16, measurement of the Rossiter-McLaughlin effect further indicates that the spin of the primary is aligned with the orbital angular momentum of the binary (Winn et al. 2011). A natural question arises: do misaligned ( $\Theta \gtrsim 5^\circ$ ) circumbinary planetary systems exist? If so, under what conditions can they form?

One might expect that circumbinary systems naturally form with highly aligned orbits, since the associated orbital angular momenta originate from the protostellar cores. However, several lines of evidence suggest that

misaligned configurations may be present in some systems:

(i) Solar-type main-sequence binaries with large separations ( $\gtrsim 40$  AU) often have a rotation axis misaligned relative to the orbital angular momentum (Hale 1994). Misalignments are also observed in some short-period binaries, such as DI Hercules (with orbital period of 10 days; Albrecht et al. 2009; see also Albrecht et al. 2011; Konopacky et al. 2012; Triaud et al. 2012).

(ii) Some binary young stellar objects (YSOs) are observed to contain circumstellar disks that are misaligned with the binary orbital plane (e.g., Stapelfeldt et al. 1998). Also, several unresolved YSOs or pre-main sequence binaries have jets along different directions, again suggesting misaligned disks (e.g., Davis, Mundt & Eislöffel 1994; Roccatagliata et al. 2011).

(iii) Imaging of circumbinary debris disks shows that the disk plane and the binary orbital plane are aligned for some systems (such as  $\alpha$  CrB,  $\beta$  Tri and HD 98800), and misaligned for others (such as 99 Herculis, with mutual inclination  $\gtrsim 30^\circ$ ; see Kennedy et al. 2012a,b). Also, the pre-main sequence binary KH 15D is surrounded by a precessing circumbinary disk inclined with respect to the binary plane by  $10^\circ$ - $20^\circ$  (e.g., Winn et al. 2004; Chiang & Murray-Clay 2004; Capelo et al. 2012), and the FS Tauri circumbinary disk appears to be misaligned with the circumstellar disk (Hioki et al. 2011).

While the aforementioned “misalignments” may have various origins (e.g., dynamical interactions in few body systems), in this paper we focus on the possible existence of warped, misaligned disks around proto-stellar binaries. We consider scenarios for the assembly of circumbinary disks in the context of binary star formation (Section

2). These scenarios suggest that circumbinary disks may form with misaligned orientations with respect to the binary. We then study the mutual gravitational interaction between the misaligned disk and the binary (Section 3) and the long-term evolution of the binary-disk systems (Section 4). We discuss our results in Section 5 and conclude in Section 6.

## 2. FORMATION OF BINARIES AND CIRCUMBINARY DISKS: SCENARIOS

Binary stars are thought to form by fragmentation inside the collapsing cores/clumps of molecular clouds, either due to turbulent fluctuation in the core (“turbulent fragmentation”; e.g., Goodwin et al. 2007; Offner et al. 2010) or due to gravitational instability in the resulting disk (“disk fragmentation”; e.g., Adams et al. 1989; Kratter et al. 2008). In the turbulent fragmentation scenario, the binaries form earlier and have initial separations of order 1000 AU. Disk fragmentation also leads to binaries with large initial separations ( $\sim 100$  AU). In both cases, continued mass accretion and inward migration, either due to binary-disk interactions (e.g., Artymowicz & Lubow 1996) or dynamical interactions in few-body systems, are needed in order to produce close (sub-AU) binaries. Planet formation can take place in the circumbinary disk during or after the binary orbital decay.

In the simplest picture, the proto-binary and circumbinary disk rotate in the same direction. However, molecular clouds and their collapsing cores are turbulent (see McKee & Ostriker 2007; Klessen 2011). It is natural that the condensing and accreting cores contain gas which rotates around different directions. Even if the cores are not turbulent, tidal torques between neighboring cores in a crowded star formation region can change the rotation direction of the outer regions of the condensing/accreting cores. Thus the gas that falls onto the central protostellar core and assembles onto the disk at different times may rotate in different directions. Such “chaotic” star formation has been seen in some numerical simulations (Bate et al. 2003). In this scenario, it is reasonable to expect a rapidly rotating central proto-stellar core which fragments into a binary, surrounded by a misaligned circumbinary disk which forms as a result of continued gas accretion.

The mutual gravitational interaction between a proto-binary and the circumbinary disk leads to secular evolution of the relative inclination between the disk and the binary plane. In most cases, this interaction, combined with continued mass accretion, tends to reduce the misalignment. We will address these issues in the next two sections. Note that previous works have focused on warped *circumstellar* disks inclined relative to the binary (e.g., Papaloizou & Terquem 1995; Bate et al. 2000; Lubow & Ogilvie 2000). The warped/twisted circumbinary disks studied below have qualitatively different behaviours.

## 3. WARPED CIRCUMBINARY DISKS

### 3.1. Disk-Binary Interaction

Consider a circumbinary disk surrounding a stellar binary. The two stars have masses  $M_1$  and  $M_2$ , and are assumed to have a circular orbit of semi-major axis  $a$ . The circumbinary disk has surface density  $\Sigma(r)$ , and extends

from  $r_{\text{in}}$  to  $r_{\text{out}}$  ( $\gg r_{\text{in}}$ ). The inner disk is truncated by the tidal torque from the binary, and typically  $r_{\text{in}} \sim 2a$  (Artymowicz & Lubow 1994; MacFadyen & Milosavljevic 2008). The orientation of the disk at radius  $r$  (from the center of mass of the binary) is specified by the unit normal vector  $\hat{\mathbf{l}}(r)$ . Averaging over the binary orbital period and the disk azimuthal direction, the binary imposes a torque per unit area on the disk element at radius  $r$  given, to leading order in  $a/r$ , by

$$\mathbf{T}_b = -\frac{3}{4} \frac{GM_t \eta \Sigma a^2}{r^3} (\hat{\mathbf{l}}_b \cdot \hat{\mathbf{l}}) (\hat{\mathbf{l}}_b \times \hat{\mathbf{l}}), \quad (1)$$

where  $M_t = M_1 + M_2$  is the total mass,  $\eta = M_1 M_2 / M_t^2$  the symmetric mass ratio of the binary, and  $\hat{\mathbf{l}}_b$  is the unit vector along the orbital angular momentum of the binary.<sup>1</sup> Under the influence of this torque, the angular momentum of an isolated disk element would precess at the frequency  $-\Omega_p \cos \beta$ , where  $\beta$  is the angle between  $\hat{\mathbf{l}}_b$  and  $\hat{\mathbf{l}}$ , and

$$\Omega_p(r) \simeq \frac{3\eta a^2}{4 r^2} \Omega(r), \quad (2)$$

with  $\Omega(r) \simeq \Omega_K = (GM_t/r^3)^{1/2}$  the disk rotation rate. Since  $\Omega_p$  depends on  $r$ , the differential precession can lead to the warping (change with  $r$  of the angle between  $\hat{\mathbf{l}}$  and  $\hat{\mathbf{l}}_b$ ) and twisting (change of  $\hat{\mathbf{l}}$  orthogonal to the  $\hat{\mathbf{l}} - \hat{\mathbf{l}}_b$  plane) of the disk.

### 3.2. Dynamical Warp Equations for Low-Viscosity disks

Theoretical studies of warped disks (Papaloizou & Pringle 1983; Papaloizou & Lin 1995) have shown that there are two dynamical regimes for the linear propagation of warps in an accretion disk. For high viscosity Keplerian disks with  $\alpha \gtrsim \delta \equiv H/r$  (where  $H$  is the half-thickness of the disk, and  $\alpha$  is the Shakura-Sunyaev parameter such that the viscosity is  $\nu = \alpha H^2 \Omega$ ), the warp satisfies a diffusion-type equation with diffusion coefficient  $\nu_2 = \nu/(2\alpha^2)$ . For low-viscosity disks ( $\alpha \lesssim \delta$ ), on the other hand, the warp propagates as bending waves at about half the sound speed,  $c_s/2$ . Protoplanetary disks with  $\alpha \sim 10^{-4}$ - $10^{-2}$  likely satisfy  $\alpha \lesssim \delta$  (e.g., Terquem 2008; Bai & Stone 2011). For such disks, the warp evolution equations governing long-wavelength bending waves in the linear regime ( $|\partial \hat{\mathbf{l}}/\partial \ln r| \ll 1$ ) are given by (Lubow & Ogilvie 2000; see also Lubow et al. 2002, Ogilvie 2006)

$$\Sigma r^2 \Omega \frac{\partial \hat{\mathbf{l}}}{\partial t} = \frac{1}{r} \frac{\partial \mathbf{G}}{\partial r} + \mathbf{T}_b, \quad (3)$$

$$\frac{\partial \mathbf{G}}{\partial t} = \left( \frac{\Omega^2 - \Omega_r^2}{2\Omega} \right) \hat{\mathbf{l}} \times \mathbf{G} - \alpha \Omega \mathbf{G} + \frac{\Sigma H^2 \Omega_z^2 r^3 \Omega}{4} \frac{\partial \hat{\mathbf{l}}}{\partial r} \quad (4)$$

where  $\Omega_r$  and  $\Omega_z$  are the radial epicyclic frequency and the vertical oscillation frequency,  $\mathbf{G}$  is the internal torque of the disk, and the surface density  $\Sigma(r)$  is taken to be the same as that of the unwrapped disk. These equations

<sup>1</sup> A similar calculation, but for the tidal torques imposed on a circumstellar disk by a binary companion, can be found in Appendix B of Ogilvie & Dubus (2001). For circumbinary disks, the only differences are that we expand the gravitational potential of the stars to first order in  $a/r$  instead of  $r/a$ , and consider the motion of both stars around the center of mass of the system instead of the motion of the companion relative to the primary star.

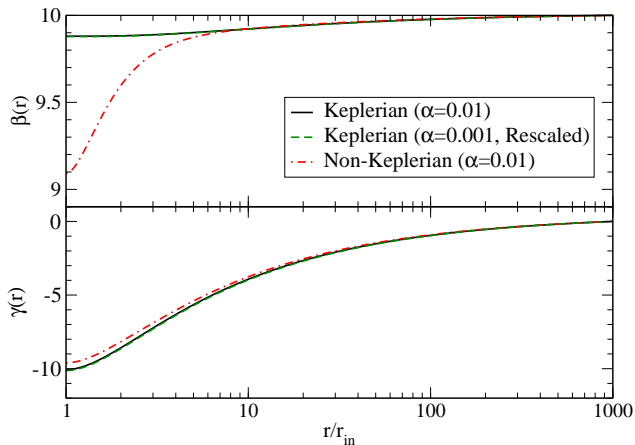


FIG. 1.— Steady-state warp (*top panel*) and twist (*bottom panel*) profiles, in degrees, of a circumbinary disk for which the outer disk is misaligned by  $10^\circ$  with respect to the angular momentum axis of the binary. Both stars in the binary have the same mass, and the disk parameters are  $p = 0.5$  [See Eq. (9)],  $\delta = 0.1$ ,  $r_{\text{in}} = 2a$ , and  $\alpha = 0.01$  or  $\alpha = 0.001$ . The profiles for  $\alpha = 0.001$  are rescaled to show the approximate scaling of the warp and twist with  $\alpha$  (i.e. the warp is multiplied by 100 and the twist by 10). Note that the rescaled  $\alpha = 0.001$  profiles nearly coincide with the  $\alpha = 0.01$  Keplerian profiles. For  $\alpha = 0.01$ , we show both the Keplerian profile, and results including the leading order non-Keplerian correction. The non-Keplerian term significantly increases the warp of the disk, but has only a small effect on its twist.

are only valid for  $\alpha \lesssim \delta \ll 1$ ,  $|\Omega_r^2 - \Omega^2| \lesssim \Omega^2 \delta$  and  $|\Omega_z^2 - \Omega^2| \lesssim \Omega^2 \delta$ . For circumbinary disks considered here, the rotation rate differs from the Keplerian rate by an amount  $|\Omega^2 - \Omega_K^2|/\Omega_K^2 = \mathcal{O}(\eta a^2/r^2) + \mathcal{O}(\delta^2)$ , and similarly for  $\Omega_r$  and  $\Omega_z$  (see Eqs (17)-(18) below). So the validity of equations (3)-(4) requires  $\eta a^2/r^2 \lesssim \delta$ , a condition that is generally satisfied.

In the absence of the external torque ( $\mathbf{T}_b = 0$ ), equations (3)-(4) admit wave solutions. If we define a Cartesian coordinate system so that  $\hat{l}_z \simeq 1$  and  $|\hat{l}_{x,y}| \ll 1$ , then a local (WKB) bending wave with  $\hat{l}_{x,y}, \mathbf{G} \propto e^{ikr - i\omega t}$  has a phase velocity  $\omega/k \simeq \pm c_s/2 = \pm H\Omega/2$  (assuming  $\omega \ll \Omega \simeq \Omega_r \simeq \Omega_z$ ).

### 3.3. Steady-State Warp and Twist of Circumbinary disks

We now consider a circumbinary disk whose rotation axis at the outer radius ( $r_{\text{out}}$ ),  $\hat{l}_{\text{out}} = \hat{l}(r_{\text{out}})$ , is inclined relative to the binary direction  $\hat{l}_b$  by a finite angle,  $\beta(r_{\text{out}}) \equiv \Theta$ . This corresponds to the situation where the outer disk region is fed by gas rotating around the axis  $\hat{l}_{\text{out}}$ . In the Cartesian coordinate system with the  $z$ -axis along  $\hat{l}_b$ , the disk direction  $\hat{l}(r)$  can be written as

$$\hat{l}(r) = (\sin \beta \cos \gamma, \sin \beta \sin \gamma, \cos \beta), \quad (5)$$

where  $\beta(r)$  is the warp angle and  $\gamma(r)$  is the twist angle. At  $r = r_{\text{out}}$ , we have  $\hat{l}_{\text{out}} = (\sin \Theta, 0, \cos \Theta)$  without loss of generality. A steady-state warp/twist is reached after a few bending wave propagation times across the whole disk. The steady-state warp/twist profile can be obtained by numerically integrating Eqs. (3)-(4) and setting  $\partial/\partial t = 0$ . Figure 1 depicts selected numerical results.

Physically, the steady-state warp/twist profile is determined by balancing the internal viscous torque  $\mathbf{G}$  of

the disk and the external torque  $\mathbf{T}_b$ . The viscous damping time of the disk warp [associated with the viscosity  $\nu_2 = \nu/(2\alpha^2)$ ] is

$$t_{v2} = \frac{r^2}{\nu_2} = \frac{2\alpha^2 r^2}{\nu} = \frac{2\alpha}{\delta^2 \Omega}. \quad (6)$$

A critical warp radius  $r_{\text{warp}}$  is obtained by equating  $t_{v2}$  to the precession time  $\Omega_p^{-1}$  of an isolated disk element, i.e.  $t_{v2}\Omega_p = 1$  at  $r = r_{\text{warp}}$  where

$$t_{v2}\Omega_p = \frac{3\alpha\eta}{2} \left(\frac{a}{r\delta}\right)^2. \quad (7)$$

This gives

$$r_{\text{warp}} \approx a \left(\frac{3\alpha\eta}{2\delta^2}\right)^{1/2}. \quad (8)$$

For  $r_{\text{warp}} \gg r_{\text{in}}$ , we expect that, in steady state, the disk well inside  $r_{\text{warp}}$  be aligned with the binary  $\hat{l}_b$ , while the disk well outside  $r_{\text{warp}}$  be aligned with  $\hat{l}_{\text{out}}$ . However, if the inner disk radius  $r_{\text{in}}$  is larger than  $r_{\text{warp}}$ , or  $(t_{v2}\Omega_p)_{\text{in}} \lesssim 1$  (the subscript “in” means that the quantity is evaluated at  $r = r_{\text{in}}$ ), then the whole disk can be approximately aligned with  $\hat{l}_{\text{out}}$ , with very small warp between the inner and outer edge of the disk. For standard disk parameters (e.g.,  $\eta \sim 1/4$ ,  $\alpha \sim 10^{-2}$ ,  $\delta \sim 0.1$ ,  $r_{\text{in}} \sim 2a$ ), the inequality  $(t_{v2}\Omega_p)_{\text{in}} \lesssim 1$  or  $r_{\text{warp}} \lesssim r_{\text{in}}$  is well satisfied.

Equation (4) shows that, to first order, changes in the orientation  $\hat{l}(r)$  of the disk are due to the combination of a term proportional to the internal stress  $\mathbf{G}$  (which modifies the twist  $\gamma$  of the disk), and a term proportional to  $\mathbf{G} \times \hat{l}$  (which causes variations of the warp  $\beta$ ). The second term only exists for non-Keplerian disks, while the first is only slightly modified by deviations from a Keplerian profile. We treat these two effects separately by first considering purely Keplerian disk profiles, to obtain a good approximation for the twist  $\gamma(r)$  in the disk, and then including non-Keplerian effects, which are generally the main source of the warp  $\beta(r)$ .

For Keplerian disks ( $\Omega_r = \Omega_z = \Omega$ ) and small warps, we can obtain approximate, analytic expressions for the disk warp and twist (see Foucart & Lai 2011 for a similar calculation of magnetically driven warped disks). For concreteness, we consider disk models with constant  $\alpha$ , and assume that the surface density and the dimensionless disk thickness have the power-law profiles

$$\Sigma \propto r^{-p}, \quad \delta = \frac{H}{r} \propto r^{(2p-1)/4}, \quad (9)$$

so that  $\dot{M} \sim \nu \Sigma = \alpha H^2 \Omega \Sigma = \text{constant}^2$ . Equations (3)-(4) then reduce to

$$\frac{\partial}{\partial r} \left[ \left(\frac{r}{r_{\text{in}}}\right)^{3/2} \frac{\partial \hat{l}}{\partial r} \right] = -\frac{4\alpha r \mathbf{T}_b}{(\delta^2 r^5 \Sigma \Omega^2)_{\text{in}}}. \quad (10)$$

<sup>2</sup> In practice, these scalings are unlikely to be valid for the entire radial extent of the disk. As the warp and twist of the disk are mostly due to the torque acting at small radii ( $\mathbf{T}_b \propto r^{-3-p}$ ), we are only concerned about the approximate value of  $p$  for  $r$  close to  $r_{\text{in}}$ .

We adopt the zero-torque boundary condition  $\partial \hat{\mathbf{l}}/\partial r = 0$  at the inner disk radius  $r = r_{\text{in}}$ . Since  $\mathbf{T}_b$  falls off rapidly with  $r$  as  $\mathbf{T}_b \propto r^{-3-p}$ , we can integrate Eq. (10) approximately to obtain:

$$\left(\frac{r}{r_{\text{in}}}\right)^{3/2} \frac{\partial \hat{\mathbf{l}}}{\partial r} \simeq \frac{4\alpha}{1+p} \left(\frac{\mathbf{T}_b}{\delta^2 r^3 \Sigma \Omega^2}\right)_{\text{in}} \left[\left(\frac{r_{\text{in}}}{r}\right)^{1+p} - 1\right]. \quad (11)$$

Using the outer boundary condition  $\hat{\mathbf{l}}(r_{\text{out}}) = \hat{\mathbf{l}}_{\text{out}}$ , we find

$$\begin{aligned} \hat{\mathbf{l}}(r) - \hat{\mathbf{l}}_{\text{out}} &\simeq \left(\frac{8\alpha}{1+p}\right) \frac{\mathbf{T}_b(r)}{(\delta^2 r^2 \Sigma \Omega^2)_{\text{in}}} \left(\frac{r}{r_{\text{in}}}\right)^{3/2} F_p(r) \\ &= -\frac{4t_{v2}\Omega_p}{(1+p)} F_p(r) (\hat{\mathbf{l}}_b \cdot \hat{\mathbf{l}}) (\hat{\mathbf{l}}_b \times \hat{\mathbf{l}}), \end{aligned} \quad (12)$$

where

$$F_p(r) = \left(\frac{r}{r_{\text{in}}}\right)^{p+1} - \frac{1}{2p+3}, \quad (13)$$

and  $t_{v2}\Omega_p$  is given by Eq. (7). In deriving Eq. (12), we have assumed that the warp and twist of the disk are small compared to its inclination relative to the binary axis, i.e.,  $|\hat{\mathbf{l}}(r) - \hat{\mathbf{l}}_{\text{out}}| \ll \sin \beta$ , or  $(t_{v2}\Omega_p)_{\text{in}} \ll 1$ . The total change in  $\hat{\mathbf{l}}$  across the disk is then

$$\hat{\mathbf{l}}_{\text{in}} - \hat{\mathbf{l}}_{\text{out}} \simeq -\frac{8(t_{v2}\Omega_p)_{\text{in}}}{2p+3} (\hat{\mathbf{l}}_b \cdot \hat{\mathbf{l}}_{\text{out}}) (\hat{\mathbf{l}}_b \times \hat{\mathbf{l}}_{\text{out}}). \quad (14)$$

The net twist angle across the disk,  $\Delta\gamma_{\text{twist}} \equiv \gamma_{\text{in}} - \gamma_{\text{out}}$ , is

$$\begin{aligned} \Delta\gamma_{\text{twist}} &\simeq -\frac{8(t_{v2}\Omega_p)_{\text{in}}}{(2p+3)} \cos \Theta \\ &= -\frac{12}{(2p+3)} \left(\frac{\alpha\eta}{\delta_{\text{in}}^2}\right) \left(\frac{a}{r_{\text{in}}}\right)^2 \cos \Theta. \end{aligned} \quad (15)$$

For Keplerian disks, the warping is only a second-order effect: to first order  $\hat{\mathbf{l}}_{\text{in}} - \hat{\mathbf{l}}_{\text{out}}$  is perpendicular to  $\hat{\mathbf{l}}_{\text{out}}$ , and the disk is only twisted. The torque acting on the inner disk does however have a component in the  $\hat{\mathbf{l}}_b - \hat{\mathbf{l}}_{\text{out}}$  plane, due to the small difference in orientation between  $\hat{\mathbf{l}}_{\text{in}}$  and  $\hat{\mathbf{l}}_{\text{out}}$ . The net warp angle,  $\Delta\beta_{\text{warp}} \equiv \beta_{\text{in}} - \beta(r_{\text{out}}) = \beta_{\text{in}} - \Theta$ , is given by

$$\begin{aligned} \Delta\beta_{\text{warp}} &\simeq -\left[\frac{4(t_{v2}\Omega_p)_{\text{in}}}{2p+3}\right]^2 \sin(2\Theta) \\ &= -\left[\frac{6}{2p+3} \left(\frac{\alpha\eta}{\delta_{\text{in}}^2}\right) \left(\frac{a}{r_{\text{in}}}\right)^2\right]^2 \sin(2\Theta). \end{aligned} \quad (16)$$

As noted before, these expressions for  $\Delta\gamma_{\text{twist}}$  and  $\Delta\beta_{\text{warp}}$  are valid only for  $|\Delta\gamma_{\text{twist}}| \ll 1$ , or  $(t_{v2}\Omega_p)_{\text{in}} \ll 1$ .

Figure 1 shows that the numerically integrated disk profile agrees with both the analytic amplitudes of the warp and twist and their scaling with the viscosity parameter  $\alpha$ . Thus, for standard disk and binary parameters ( $\eta = 0.25$ ,  $\alpha = 10^{-3}$ - $10^{-2}$ ,  $\delta = 0.1$  and  $r_{\text{in}} \simeq 2a$ ), the steady-state Keplerian disk is almost flat, with its orientation determined by  $\hat{\mathbf{l}}_{\text{out}}$ , i.e., the angular momentum axis of the gas falling onto the outer disk.

Deviations from a Keplerian disk profile modify the above results, as differences between the epicyclic and

orbital frequency of the disk are induced by both the finite thickness of the disk and the deviation of the binary gravitational potential from its point-mass value. To first order in  $\delta^2$  and  $\eta(a/r)^2$ , we have (assuming small binary-disk inclination  $\Theta$ )

$$\Omega^2 \approx \frac{GM_t}{r^3} \left(1 + \frac{3\eta a^2}{4r^2} - C\delta^2\right) \quad (17)$$

$$\Omega_r^2 \approx \frac{GM_t}{r^3} \left(1 - \frac{3\eta a^2}{4r^2} - D\delta^2\right) \quad (18)$$

where  $C$  and  $D$  are constants of order unity which depend on the density/pressure profile of the disk, and the epicyclic frequency was computed from  $\Omega_r^2 = (2\Omega/r)d(r^2\Omega)/dr$ . We thus have

$$\frac{\Omega^2 - \Omega_r^2}{\Omega^2} \approx \frac{3\eta a^2}{2r^2} + (D - C)\delta^2. \quad (19)$$

It is worth noting that for  $\delta = \text{constant}$ , the  $\delta^2$  term vanishes (since  $C = D$  in that case). Including this result in Eq. (4) leads to an additional warp

$$\Delta\beta_{\text{warp}}^{\text{NK}} \approx -K \frac{\eta}{\delta_{\text{in}}^2} \left(\frac{a}{r_{\text{in}}}\right)^2 \sin(2\Theta) \quad (20)$$

with

$$K = \frac{0.9\eta}{2p+7} \left(\frac{a}{r_{\text{in}}}\right)^2 + \kappa\delta_{\text{in}}^2 \quad (21)$$

and  $\kappa$  a constant depending on the profile of  $\delta(r)$  close to  $r_{\text{in}}$  ( $\kappa = 0$  for constant  $\delta$ , and of order unity for slowly varying  $\delta$ ). Numerical results for the non-Keplerian steady-state disk profile are shown in Figure 1 for constant thickness  $\delta$ . We see that even though the warp remains relatively small ( $\Delta\beta_{\text{warp}}^{\text{NK}} \sim 0.1\beta$ ), for  $\alpha \lesssim 0.03$  it will be larger than the second-order Keplerian warp given by Eq. (16). As most of the torque on the disk is due to the contributions at radii  $r \sim r_{\text{in}}$ , this warp also causes a reduction of the Keplerian twist  $\Delta\gamma_{\text{twist}}$  [See Eq. (15)] by a factor of order  $(\sin \beta_{\text{in}}/\sin \beta_{\text{out}})$ .

#### 4. EVOLUTION OF THE RELATIVE BINARY - DISK INCLINATION

As discussed in Section 3, the binary torque [Eq. (1)] induces a small warp and twist in the circumbinary disk. For disks satisfying  $\delta \gtrsim \alpha$ , the steady-state warp/twist is achieved when transient bending waves either damp out or propagate out of the disk (depending on their behavior at large radius). Bending waves propagate at half the sound speed, and will thus reach the outer boundary of the disk over a timescale

$$t_{\text{warp}} \sim \int_{r_{\text{in}}}^{r_{\text{out}}} \frac{dr}{H\Omega/2} \sim \frac{2}{\delta_{\text{out}}\Omega_{\text{out}}}. \quad (22)$$

As for the damping of transient bending waves, it is due to the  $\alpha\Omega\mathbf{G}$  term in Eq. (4). Numerical results (Lubow & Ogilvie 2000) have confirmed that the damping timescale is

$$t_{\text{damp}} \sim \frac{1}{\alpha\Omega_{\text{out}}}. \quad (23)$$

Both timescales are much shorter than the age of the system or the gas accretion time

$$t_{\text{acc}} \sim \left(\frac{r^2}{\nu}\right)_{\text{out}} \sim \frac{1}{\alpha \delta_{\text{out}}^2 \Omega_{\text{out}}}. \quad (24)$$

On a timescale longer than  $t_{\text{damp}}$ , the warped disk exerts a back-reaction torque on the binary, aligning  $\hat{\mathbf{l}}_b$  with the disk axis (more precisely, with  $\hat{\mathbf{l}}_{\text{out}}$ ). To determine this torque, recall that in the Cartesian coordinate system that we have set up,  $\hat{\mathbf{l}}_b = (0, 0, 1)$  and  $\hat{\mathbf{l}}_{\text{out}} = (\sin \Theta, 0, \cos \Theta)$ . In the small-warp approximation,  $\hat{\mathbf{l}}(r) \simeq (\sin \Theta + \Delta \hat{l}_x, \Delta \hat{l}_y, \cos \Theta)$ , where  $\Delta \hat{l}_{x,y}$  are the  $(x,y)$ -components of  $\hat{\mathbf{l}}(r) - \hat{\mathbf{l}}_{\text{out}}$ .  $\Delta \hat{l}_y$  is well approximated by [see Eq. (12)]

$$\Delta \hat{l}_y \simeq -\frac{4 t_{v2} \Omega_p}{(1+p)} F_p(r) \cos \Theta \sin \Theta, \quad (25)$$

and thus  $|\Delta \hat{l}_y| \ll \sin \Theta$  when  $t_{v2} \Omega_p \ll 1$ .  $\Delta \hat{l}_x$  is mainly due to non-Keplerian effects [see Eq. (20)], and is generally a small correction ( $\sim 10\%$ ) to  $\sin \Theta$ . Thus the torque on the disk element [Eq. (1)] is, to leading order for each component,

$$\mathbf{T}_b \simeq -\frac{3 GM_t \eta \Sigma a^2}{4 r^3} \cos \Theta \left(-\Delta \hat{l}_y, \sin \Theta, 0\right). \quad (26)$$

The back-reaction torque on the binary is

$$\mathcal{T} = -\int_{r_{\text{in}}}^{r_{\text{out}}} 2\pi r \mathbf{T}_b dr \quad (27)$$

The  $x$ -component of  $\mathcal{T}$  tends to align  $\hat{\mathbf{l}}_b$  with  $\hat{\mathbf{l}}_{\text{out}}$ :

$$\mathcal{T}_x \simeq \frac{72\pi}{(2p+3)(4p+5)} \left(\frac{\alpha \eta^2}{\delta_{\text{in}}^2}\right) a^4 \Sigma_{\text{in}} \Omega_{\text{in}}^2 \cos^2 \Theta \sin \Theta. \quad (28)$$

If we define the angular momentum of the inner disk region by

$$(\Delta J)_{\text{in}} \equiv 2\pi (\Sigma r^4 \Omega)_{\text{in}}, \quad (29)$$

then  $\mathcal{T}_x$  can be written as

$$\mathcal{T}_x = \frac{32}{(2p+3)(4p+5)} (\Delta J)_{\text{in}} (\Omega_p^2 t_{v2})_{\text{in}}, \quad (30)$$

where  $t_{v2} \Omega_p = (3\alpha\eta/2)(a/r\delta)^2$  [see Eq. (7)].

The  $y$ -component of  $\mathcal{T}$  on the binary is

$$\mathcal{T}_y = \frac{3\pi}{2(1+p)} GM_t \eta \frac{a^2 \Sigma_{\text{in}}}{r_{\text{in}}} \cos \Theta \sin \Theta. \quad (31)$$

This makes the binary axis  $\hat{\mathbf{l}}_b$  precess around  $\hat{\mathbf{l}}_{\text{out}}$  at the rate

$$\Omega_{\text{prec}} = -\frac{3\pi}{2(1+p)} \left(\frac{\Sigma_{\text{in}} a^3}{M_t r_{\text{in}}}\right) \Omega_b \cos \Theta \hat{\mathbf{l}}_{\text{out}}, \quad (32)$$

where  $\Omega_b = (GM_t/a^3)^{1/2}$  is the orbital frequency of the binary. Since  $\mathcal{T}_y$  does not induce permanent change of the inclination angle  $\Theta$ , we will not consider it further in this paper.

It is worth noting that to leading order the back-reaction torque is independent of the non-Keplerian warp computed in Eq. (20), even when that warp is the main

deviation from the flat-disk profile. Indeed,  $\mathcal{T}_x$  is proportional to the twist  $\Delta \hat{l}_y$  and  $\mathcal{T}_y$  to  $\sin \Theta$ . The only effect of the non-Keplerian warp is thus to modify  $\mathcal{T}$  by a factor of order  $(\sin \beta_{\text{in}}/\sin \beta_{\text{out}})$ .

Mass accretion from the circumbinary disk onto the binary can also contribute to the alignment torque. The accretion streams from  $r_{\text{in}}$  will likely land in both stars, probably through circumstellar disks (e.g., Artymowicz & Lubow 1994; MacFadyen & Milosavljevic 2008). Given the complexity of the process, we parametrize the alignment torque due to accretion as

$$\mathcal{T}_{\text{acc},x} = g \dot{M} (GM_t r_{\text{in}})^{1/2} \sin \Theta, \quad (33)$$

where  $g$  is a dimensionless number of order unity. In writing Eq. (33), we have used the result of Section 3 that the steady-state circumbinary disk is only slightly warped [ $\beta(r_{\text{in}}) \simeq \Theta$ ]. Since the mass accretion rate is given by  $\dot{M} \simeq 3\pi\nu\Sigma = 3\pi\alpha(\delta^2 r^2 \Omega\Sigma)_{\text{in}}$ , we can rewrite Eq. (28) as

$$\mathcal{T}_x \simeq f \dot{M} (GM_t r_{\text{in}})^{1/2} \cos^2 \Theta \sin \Theta, \quad (34)$$

where

$$f = \frac{24}{(2p+3)(4p+5)} \eta^2 \left(\frac{a}{\delta_{\text{in}} r_{\text{in}}}\right)^4. \quad (35)$$

The total alignment torque on the binary is then

$$\begin{aligned} \mathcal{T}_{\text{align}} &= \mathcal{T}_{\text{acc},x} + \mathcal{T}_x \\ &\simeq (g + f \cos^2 \Theta) \dot{M} (GM_t r_{\text{in}})^{1/2} \sin \Theta. \end{aligned} \quad (36)$$

Assuming that the angular momentum of the binary,  $L_b = \eta M_t (GM_t a)^{1/2}$ , is much less than that of the disk (and the material falling onto the disk), the torque  $\mathcal{T}_{\text{align}}$  leads to alignment between  $\hat{\mathbf{l}}_b$  and  $\hat{\mathbf{l}}_{\text{out}}$ , on the timescale

$$t_{\text{align}} = \frac{L_b \sin \Theta}{\mathcal{T}_{\text{align}}} = \frac{\eta M_t}{\dot{M}} \left(\frac{a}{r_{\text{in}}}\right)^{1/2} \frac{1}{(g + f \cos^2 \Theta)}. \quad (37)$$

The secular evolution of  $\Theta(t)$  is determined by the equation

$$\frac{d\Theta}{dt} = -\frac{\sin \Theta}{t_{\text{align}}}. \quad (38)$$

For  $\Theta \ll 1$ , this can be easily solved: Starting from the initial angle  $\Theta(t_i)$ , the inclination evolves according to

$$\Theta(t) = \Theta(t_i) \exp \left[ -\frac{\Delta M}{\eta M_t} \left(\frac{r_{\text{in}}}{a}\right)^{1/2} (g + f) \right], \quad (39)$$

where  $\Delta M$  is the total mass accreted through the disk during the time between  $t_i$  and  $t$ .

## 5. DISCUSSION

The calculations presented in Sections 3 and 4 show that a circumbinary disk formed with its rotation axis  $\hat{\mathbf{l}}_{\text{out}}$  (at large distance) inclined with respect to the binary angular momentum axis  $\hat{\mathbf{l}}_b$  will attain a weakly warped/twisted state, such that the whole disk is nearly aligned with  $\hat{\mathbf{l}}_{\text{out}}$  (see Section 3). However, the interaction torque between the disk and the binary tends to drive  $\hat{\mathbf{l}}_b$  toward alignment with  $\hat{\mathbf{l}}_{\text{out}}$ . The timescale of this

alignment is given by Eq. (37), and the relative binary-disk inclination  $\Theta$  evolves according to Eq. (39).

Note that both the accretion torque and the gravitational torque contribute to the alignment. If only the accretion torque were present (i.e.,  $g \sim 1$ ,  $f = 0$ ), the alignment timescale would be of the same order as the mass-doubling time of the binary ( $t_{\text{align}} \sim 4 \times 10^7$  yr for  $M_1 = M_2 = 1 M_\odot$ ,  $r_{\text{in}} \simeq 2a$  and  $\dot{M} \sim 10^{-8} M_\odot \text{yr}^{-1}$ ), and a significant fraction of the binary mass would have to be accreted ( $\Delta M \sim 0.4 M_\odot$ ) in order to achieve an  $e$ -fold reduction of  $\Theta$  [see Eq. (39)]. However, the gravitational torque dominates over the accretion torque, since the condition  $f \gg 1$  can be satisfied for a wide range of disk/binary parameters (although  $\alpha^2 f \ll 1$  must be satisfied for our equations to be valid). For example, for  $p = 3/2$  (the density index for the minimum solar nebula), and  $\eta = 1/4$  (equal mass binary), we have

$$f \simeq 14 \left( \frac{0.1}{\delta_{\text{in}}} \right)^4 \left( \frac{2a}{r_{\text{in}}} \right)^4. \quad (40)$$

Thus, the alignment timescale is (for  $f \gg 1$  and  $\cos^2 \Theta \simeq 1$ )

$$t_{\text{align}} \simeq 2.5 \left( \frac{\eta M_t}{0.5 M_\odot} \right) \left( \frac{\dot{M}}{10^{-8} M_\odot/\text{yr}} \right)^{-1} \left( \frac{\delta_{\text{in}}}{0.1} \right)^4 \left( \frac{r_{\text{in}}}{2a} \right)^{3.5} \text{ Myrs} \quad (41)$$

( $\eta M_t$  is the reduced mass of the binary). The amount of mass accretion needed for an  $e$ -fold reduction of  $\Theta$  is [see Eq. (39)]

$$(\Delta M)_e \simeq 0.05 (\eta M_t) \left( \frac{\delta_{\text{in}}}{0.1} \right)^4 \left( \frac{r_{\text{in}}}{2a} \right)^{3.5}. \quad (42)$$

Thus, only a small fraction of the binary mass has to be accreted to achieve significant reduction of  $\Theta$ .

We comment on two assumptions adopted in our calculations of Sections 3-4:

(i) We have assumed that the binary separation  $a$  is constant. In reality, the binary-disk alignment can take place simultaneously as the binary orbit shrinks (due to binary-disk interactions). However, since the alignment timescale depends only on the ratio  $r_{\text{in}}/a$ , we expect our result to be largely unchanged in such a situation as long as  $r_{\text{in}}$  keeps track of  $a$  while the orbit decays.

(ii) We have assumed that there is a constant supply of gas at the outer disk and the total angular momentum of the disk,  $L_{\text{disk}}$ , is much larger than that of the binary,  $L_b$ . If we consider an isolated circumbinary disk (e.g., when an episode of mass infall from the turbulent cloud/core onto the central binary occurs) with  $L_{\text{disk}}$  comparable or smaller than  $L_b$ , then both the binary and the disk will precess around a common total angular momentum axis while the mutual inclination  $\Theta$  evolves. In this case, equation (38) is replaced by

$$\frac{d\Theta}{dt} = -\frac{\mathcal{T}_{\text{align}}}{L_b} - \frac{\mathcal{T}_{\text{align}}}{L_{\text{disk}}} \cos \Theta = -\frac{\sin \Theta}{t_{\text{align}}} \left( 1 + \frac{L_b \cos \Theta}{L_{\text{disk}}} \right). \quad (43)$$

This equation neglects the accretion torque, so that  $\mathcal{T}_{\text{align}} \simeq \mathcal{T}_x$ . Note that in general,  $\mathcal{T}_x$  and  $t_{\text{align}}$  will be modified from the expressions given in Section 3. But as long as  $r_{\text{out}} \gg r_{\text{in}}$ , we expect the corrections to be

small (Foucart & Lai, in preparation). It is also of interest to note that when  $\cos \Theta < -L_{\text{disk}}/L_b$ , the gravitational torque tends to drive  $\Theta$  toward  $180^\circ$  (i.e., counter-alignment). However, this criteria is only valid instantaneously: both  $L_{\text{disk}}$  and  $L_b$  vary in time due to dissipation in the disk and accretion onto the binary, and there is thus no guarantee that the evolution of  $\Theta$  is monotonic. To determine which initial conditions lead to counter-alignment, assumptions have to be made regarding the evolution of  $L_{\text{disk}}$  and  $L_b$ . King et al.(2005) showed that if  $L_b$  is constant (negligible accretion onto the binary), counter-alignment will occur if the less restrictive condition  $\cos \Theta < -L_{\text{disk}}/(2L_b)$  is satisfied — even though initially  $d\Theta/dt < 0$ .<sup>3</sup>

## 6. CONCLUSIONS AND IMPLICATIONS

In this paper, we have considered scenarios for the assembly of proto-planetary disks around newly formed stellar binaries. The shape and inclination of the disk relative to the binary will determine the orbital orientations of the circumbinary planets that are formed in the disk. Because of the turbulence in molecular clouds and dense cores, inside which protostellar binaries and circumbinary disks form, and also because of the tidal torques between nearby cores, it is possible, and even likely, that gas falling onto the outer region of the circumbinary disk rotates along a direction different from the rotation axis of the binary. Thus in general, the newly assembled circumbinary disk will be misaligned with respect to the binary. However, the gravitational torque from the binary produces a warp and twist in the disk, and the back-reaction torque associated with that twist tends to align (under most conditions) the disk and the binary orbital plane. We have presented new calculations of the interaction between the warped/twisted disk and the binary, and showed that the disk warp is small under typical conditions. More importantly, we have derived new analytic expressions for the binary-disk alignment torque and the associated timescale [see Eq. (41)]. Our results show that the misalignment angle can be reduced appreciably after the binary accretes a few percent of its reduced mass [see Eq. 42].

Proto-binaries formed by fragmentation (either turbulent fragmentation or disk fragmentation; see Section 2) have initial separations much larger than 1 AU. Significant inward migration must occur to produce close (sub-AU) binaries. Since mass accretion necessarily takes place during disk-driven binary migration, our results then suggest that close binaries are likely to have aligned circumbinary disks, while wider binaries *can* have misaligned disks. This can be tested by future observations. The circumbinary planetary systems discovered by *Kepler* (see Section 1) all contain close (period  $\lesssim 41$  d) binaries. If the planets form in the late phase of the circumbinary disk (as is likely to be the case considering the relatively small planet masses in the *Kepler* systems), then the planetary orbits will be highly aligned with the binary orbits, even if the initial disk has a misaligned orientation. This is indeed what is observed.

<sup>3</sup> King et al.(2005) studied accretion disks around spinning black holes, not circumbinary disks. However, the mathematical form of the evolution equation for  $\Theta$  is identical to the circumbinary case (compare e.g. Eq. (43) of this work with Eq.(18) of King et al.).

Of course, given the complexity of the various processes involved, one may see some exceptions. In particular, in this paper we have not considered any dynamical processes (few body interactions) that may take place after the binary and planet formation. Such processes can also affect the mutual inclinations of circumbinary planets.

Observationally, tertiary bodies on misaligned orbits around close, eclipsing binaries can be detected by searching for periodic eclipse timing variations. This has led to the identification of many binaries with tertiary companions (e.g., Liao & Qian 2010; Gies et al. 2012). A number of post-main-sequence eclipsing binaries have been claimed to host candidate circumbinary planets, such as HW Virginis (Lee et al. 2009), HU Aquarii (Qian et al. 2011; Gozdziewski et al. 2012), NN Serpentis (Beuermann et al. 2010), DP Leonis (Beuermann et al. 2011) and NY Vir (Qian et al. 2012). However,

some of these claims are controversial since the proposed planetary orbits may be dynamically unstable on short timescales (see Horner et al. 2011, 2012). Currently, no misaligned (inclination  $\gtrsim 5^\circ$ ) circumbinary planets have been confirmed around main-sequence binaries.

Overall, our calculations in this paper illustrate that the mutual inclinations and other orbital characteristics of circumbinary planetary systems can serve as a diagnostic tool for the assembly and evolution of protoplanetary disks and the condition of formation of these planetary systems.

#### ACKNOWLEDGMENTS

This work has been supported in part by the NSF grants AST-1008245, AST-1211061 and the NASA grant NNX12AF85G.

#### REFERENCES

- Adams F.C., Ruden S.P., Shu F.H., 1989, *ApJ*, 347, 959  
 Artymowicz P., Lubow S.H. 1994, *ApJ*, 421, 651  
 Artymowicz P., Lubow S.H. 1996, *ApJ*, 467, L77  
 Albrecht, S., Reffert, S., Snellen, I.A.G., Winn, J.N. 2009, *Nature*, 461, 373  
 Albrecht, S., Winn, J.N., Carter, J.A., Snellen, I.A.G., de Mooij, E.J.W. 2011, *ApJ*, 726, 68  
 Bai, X.-N., Stone, J.M. 2011, *ApJ*, 736, 144  
 Bate, M.R., et al. 2000, *MNRAS*, 317, 773  
 Bate, M.R., Bonnell, I.A., Bromm, V. 2003, *MNRAS*, 339, 577  
 Beuermann, K., et al., 2010, *A&A*, 521, L60  
 Beuermann, K., et al., 2011, *A&A*, 526, A53  
 Capelo, H. L., et al. 2012, arXiv:1208.5497  
 Chiang, E. I., & Murray-Clay, R. A. 2004, *ApJ*, 607, 913  
 Davis, C.J., Mundt, R., Eisloffel, J. 1994, *ApJ*, 437, L58  
 Doyle, L.R., Carter, J.A., Fabrycky, D.C., Slawson, R.W., Howell, S.B., et al. 2011, *Science*, 333, 1602  
 Foucart, F., Lai, D. 2011, *MNRAS*, 412, 2799  
 Gies, D.R., et al. 2012, *ApJ*, 143, 137  
 Goodwin S.P., Kroupa P., Goodman A., Burkert A., 2007, *Protostars and Planets V* (Univ. Arizona Press), pp 1331-147  
 Gozdziewski K, et al., 2012, *MNRAS*, 425, 930  
 Hale A., 1994, *Astron. J.*, 107, no. 1, p. 306-332  
 Hioki, J. et al. 2011, *PASJ*, 63, 543:  
 Horner J., Marshall J.P., Wittenmyer R.A., Tinney C.G., 2011, *MNRAS*, 416, L11  
 Horner J., Wittenmyer R.A., Hinse T.C., Tinney C.G., 2012, *MNRAS*, 425, 749  
 Kennedy, G. M., et al. 2012a, *MNRAS*, 421, 2264  
 Kennedy, G. M., et al. 2012b, arXiv:1208.1759  
 King A.R., Lubow S.W., Ogilvie G.H., Pringle J.E., 2005, *MNRAS*, 363, 49  
 Klessen, R.S. 2011, arXiv:1109.0467  
 Konopacky, Q.M., et al. 2012, *ApJ*, 750, 79  
 Kostov V.B., et al. 2012, arXiv:1210.3850  
 Kratter K.M., Matzner C.D., Krumholz, M.R., 2008, *ApJ*, 681, 375  
 Lee, J.W., et al., 2009, *AJ*, 137, 3181  
 Liao, W.-P., Qian, S.-B. 2010, *MNRAS*, 405, 1930  
 Lubow, S. H. & Ogilvie G. I., 2000, *ApJ*, 538, 326  
 Lubow S. H., Ogilvie G. I. & Pringle, J.E. 2002, *MNRAS*, 337, 706  
 MacFadyen, A.I., Milosavljevic, M. 2008, *ApJ*, 672, 83  
 McKee C.F., Ostriker, E.C. 2007, *ARAA*, 45, 565  
 Offner S.S.R., Kratter K.M., Matzner C.D., Krumholz M.R., Klein R.I., 2010, *ApJ*, 725, 1485  
 Ogilvie G.I., 2006, *MNRAS*, 365, 977  
 Ogilvie G.I., Dubus G., 2001, *MNRAS*, 320, 485  
 Orosz, J.A., Welsh, W.F., Carter, J.A., Brugamyer, E., Buchhave, L.A. et al. 2012a, *ApJ*, 758, 87  
 Orosz, J.A., et al. 2012b, *Science*, 337, 1511  
 Papaloizou J.C.B. & Lin D.N.C., 1995, *ApJ*, 438, 841  
 Papaloizou J.C.B. & Pringle J.E., 1983, *MNRAS*, 202, 1181  
 Papaloizou, J.C.B., Terquem, C. 1995, *MNRAS*, 274, 987  
 Qian, S.-B., et al., 2011, *MNRAS*, 414, L16  
 Qian, S.-B., et al., 2012, *ApJ*, 745, L23  
 Roccatagliata, V., Ratzka, T., Henning, T., Wolf, S., Leinert, C., & Bouwman, J. 2011, *A&A*, 534, A33  
 Schwamb, M.E., et al. 2012, arXiv: 1210.3612  
 Stapelfeldt, K.R., et al. 1998, *ApJ*, 502, L65  
 Terquem C., 2008, *ApJ*, 689, 532  
 Triaud, A.H.M.J., et al. 2012, *A&A*, submitted (arXiv:1208.4940)  
 Welsh, W.F., Orosz, J.A., Carter, J.A., Fabrycky, D.C., Ford, E.B., et al. 2012 *Nature*, 481, 475  
 Winn, J.N., Holman, M.J., Johnson, J.A., Stanek, K.Z., & Garnavich, P.M. 2004, *ApJ*, 603, L45  
 Winn, J.N., et al. 2011, *ApJ*, 741, L1.